HHS Public Access

Author manuscript

Neuroscience. Author manuscript; available in PMC 2018 June 23.

Published in final edited form as:

Neuroscience. 2017 June 23; 354: 158–167. doi:10.1016/j.neuroscience.2017.04.034.

Disruption of $K_V2.1$ somato-dendritic clusters prevents the apoptogenic increase of potassium currents

Jason A. Justice*, **Anthony J. Schulien**, **Kai He**, **Karen A. Hartnett**, **Elias Aizenman**, and **Niyathi H. Shah**

Department of Neurobiology and Pittsburgh Institute for Neurodegenerative Diseases, University of Pittsburgh School of Medicine, Pittsburgh, PA, USA 15213. Tel: 412-648-9434; Fax: 412-648-1441

Abstract

As the predominant mediator of the delayed rectifier current, $K_V2.1$ is an important regulator of neuronal excitability. $K_V2.1$, however, also plays a well-established role in apoptotic cell death. Apoptogenic stimuli induce syntaxin-dependent trafficking of $K_V2.1$, resulting in an augmented delayed rectifier current that acts as a conduit for K^+ efflux required for pro-apoptotic protease/nuclease activation. Recent evidence suggests that $K_V2.1$ somato-dendritic clusters regulate the formation of endoplasmic reticulum–plasma membrane junctions that function as scaffolding sites for plasma membrane trafficking of ion channels, including $K_V2.1$. However, it is unknown whether $K_V2.1$ somato-dendritic clusters are required for apoptogenic trafficking of $K_V2.1$. By overexpression of a protein derived from the C-terminus of the cognate channel $K_V2.2$ ($K_V2.2CT$), we induced calcineurin-independent disruption of $K_V2.1$ somato-dendritic clusters in rat cortical neurons, without altering the electrophysiological properties of the channel. We observed that $K_V2.2CT$-expressing neurons are less susceptible to oxidative stress-induced cell death. Critically, expression of $K_V2.2CT$ effectively blocked the increased current density of the delayed rectifier current associated with oxidative injury, supporting a vital role of $K_V2.1$-somato-dendritic clusters in apoptogenic increases in $K_V2.1$-mediated currents.

Keywords

potassium channel; oxidative-stress; $K_V2.1$; apoptosis; zinc; syntaxin

Introduction

Numerous acute and chronic neurodegenerative processes involve progressive apoptotic neuronal cell death (Danial & Korsmeyer, 2004). Since the central nervous system has very limited regenerative capability, therapeutic approaches aimed at limiting apoptotic neuronal loss are essential. Importantly, apoptosis is regulated by numerous checkpoints that may

*Address all correspondence to: Dr. Jason A. Justice; jjustice@pitt.edu.

provide effective pharmacotherapeutic targets. Critical in the formation of the apoptosome, as well as in the activation of pro-apoptotic proteases and nucleases, K^+ efflux is a prerequisite for the completion of various apoptotic programs in many cell types, including neurons (Bortner *et al.*, 1997; Hughes *et al.*, 1997; Yu *et al.*, 1997; Hughes & Cidlowski, 1999; Montague *et al.*, 1999; Huang *et al.*, 2001; Wei *et al.*, 2004; Bortner & Cidlowski, 2007). The delayed rectifier current, predominantly mediated by $K_V2.1$ channels (Murakoshi & Trimmer, 1999; Malin & Nerbonne, 2002), has been demonstrated to perform a critical role in apoptogenic K^+ efflux in cortical, nigral, and hippocampal neurons (Pal *et al.*, 2003; Redman *et al.*, 2006; Shen *et al.*, 2009; Shepherd *et al.*, 2012). Suppressing delayed rectifier current-mediated K^+ efflux decreases cellular susceptibility to apoptotic stimuli, including oxidative stress (Yu *et al.*, 1997; Aizenman *et al.*, 2000; McLaughlin *et al.*, 2001; Wei *et al.*, 2004; Pal *et al.*, 2006; Redman *et al.*, 2007; Redman *et al.*, 2009; Norris *et al.*, 2012; Shepherd *et al.*, 2012).

$K_V2.1$ is unique among voltage-gated potassium channels in its widespread expression, subcellular localization and physiological functions. At least two distinct populations with different localization patterns exist in neurons, each serving distinct physiological roles (O'Connell *et al.*, 2006; O'Connell *et al.*, 2010; Fox *et al.*, 2013). One population is freely dispersed on the plasma membrane of neurons and is the primary mediator of the delayed rectifier current, playing an important role in regulating intrinsic neuronal excitability (Murakoshi & Trimmer, 1999; Du *et al.*, 2000; Malin & Nerbonne, 2002; O'Connell *et al.*, 2010; Fox *et al.*, 2013; Guan *et al.*, 2013). A separate neuronal population of seemingly non-conducting $K_V2.1$ channels are constrained within micron-sized clusters in the soma and proximal dendrites, regulate the formation of endoplasmic reticulum–plasma membrane junctions and serve as scaffolding sites for endo- and exocytosis of ion channels, including $K_V2.1$ (O'Connell *et al.*, 2010; Fox *et al.*, 2013). $K_V2.1$ activation and localization are highly dynamic and both are modulated by a number of stimuli, including hypoxia and ischemia (Mulholland *et al.*, 2008; Cobb *et al.*, 2015). Hypoxia/ischemia induces dephosphorylation of the channel and dispersal of somato-dendritic clusters *in vivo* as well as a hyperpolarized shift in the steady state activation, $V_{1/2}$, *in vitro* (Misonou *et al.*, 2005b). This shift in $V_{1/2}$ decreases neuronal excitability and is thought to provide neuroprotection by limiting excitotoxicity (Aras *et al.*, 2009a; Aras *et al.*, 2009b; Mohapatra *et al.*, 2009; Shepherd *et al.*, 2013). Although normally associated with the hyperpolarized shift in $V_{1/2}$, the dispersal of $K_V2.1$ somato-dendritic clusters has no known protective function.

Since apoptogenic K^+ efflux is known to involve newly inserted $K_V2.1$ channels (Pal *et al.*, 2003), we hypothesized that a lack of $K_V2.1$-containing clusters would preclude pro-apoptotic channel trafficking and rescue neurons from apoptotic stimuli. Overexpression of $K_V2.2CT$, a protein derived from the C-terminus of $K_V2.2$, induces dispersal of $K_V2.1$ somato-dendritic clusters without affecting the channel's electrophysiological properties (Baver & O'Connell, 2012). By utilizing this effect of $K_V2.2CT$ on $K_V2.1$ channel localization, we were able to explore potential neuroprotective effects mediated by $K_V2.1$ localization, separate from the dampening of neuronal excitability induced by hyperpolarized shifts in $V_{1/2}$. We report that $K_V2.2CT$-expressing neurons are less susceptible to oxidative stress-induced cell death. Critically, expression of $K_V2.2CT$ effectively blocked the increased current density of the delayed rectifier current associated

with oxidative stress-induced neuronal death, supporting a vital role of $K_V2.1$ somato-dendritic clusters in apoptogenic trafficking of $K_V2.1$.

Experimental Procedures

Cell culture and transfection procedures

Pregnant Sprague-Dawley dams were housed in a University of Pittsburgh animal care facility prior to using day 16–17 rat embryos to generate cortical cultures, as described previously (Hartnett *et al.*, 1997). At 3–4 weeks *in vitro*, cultures were transfected using Lipofectamine 2000 (Invitrogen, Carlsbad, CA) in Opti-Mem I medium with a total of 1.5 μg cDNA (Ohki *et al.*, 2001). Cells were maintained for 24–48 hours at 37°C, 5% CO_2 before electrophysiological recordings and toxicity assays were performed.

Immortalized microglial cells were generously supplied by J. Connor (Pennsylvania St. University, Hershey, PA, USA). For detailed information on cell culture procedures used for microglial cells see Knoch et al. 2008. Briefly, immortalized rat brain microglial cells (Cheepsunthorn *et al.*, 2001) were maintained in Dulbeco's modified MEM supplemented with 10% heat-inactivated fetal bovine serum, and plated at a density of 50,000 cells/well for 24 hours prior to activation (Li et al. 2005). Microglia were then added directly to cortical cultures and activated with 10 U/mL interferon-γ (Chemicon, Temecula, CA, USA) and 1 μg/mL lipopolysaccharide for 60 minutes. Co-cultures were then immediately incubated and maintained in the dark at 37° C and 5% CO_2 for 24 hours prior to luciferase viability assay experiments.

Chinese Hamster ovary (CHO) cells were maintained in F12 Nutrient medium with 10% heat-inactivated FBS and penicillin streptomycin. CHO cells were plated onto six-well plates, at 280,000 cells/well, 24 hours prior to transfection. Cells were transfected using Lipofectamine reagent (Invitrogen, Carlsbad, CA, USA) in serum-free medium with a total of 1.4 μg of cDNA per well. Cells were maintained for 24 hours at 37° C, 5% CO_2 before use in co-immunoprecipitation and western blot experiments.

Electrophysiological measurements

Whole-cell voltage-clamp currents from rat cortical neurons were obtained with Axopatch 200B amplifier and pClamp software (Molecular Devices, Sunnyvale, CA, USA) using 3–5 MΩ electrodes. Electrodes were pulled from 1.5 mm borosilicate glass (Warner Instruments, Hamden, CT, USA) with a model P-97 mechanical pipette puller (Sutter Instruments, Novato, CA, USA). The extracellular solution contained the following (in mM): 2.0 $MgCl_2$, 2.5 KCl, 115 NaCl, 10 HEPES, 10 D-glucose, 1.0 $CaCl_2$,and 0.25 μM tetrodotoxin, pH 7.2. The electrode solution contained the following (in mM): 100 K-gluconate, 1 $MgCl_2$, 10 KCl, 1 $CaCl_2$, 2.2 $MgCl_2$. ATP, 0.33 GTP, 11 EGTA, and 10 HEPES, pH 7.2. In all cases, series resistance was partially compensated (80%). Currents were digitized at 10 kHz and filtered at 2 kHz. K^+ currents were evoked with a series of 200 ms voltage steps from a holding potential of −80 to +80 mV in 10 mV increments. A single 30 ms prepulse to +10 mV was used before depolarization in order to inactivate A-type K^+ currents. Delayed rectifier currents were measured relative to baseline at 180 milliseconds after the initiation of each

voltage step. Currents were then normalized to cell capacitance or maximal conductance. Peak conductance (G) was calculated from peak steady-state current amplitudes (I) using the equation G = I/(V − EK) (EK = Nernst K^+ equilibrium potential) and plotted against the potential (V), then fitted to a single Boltzmann function, $G = G_{max}/(1 + \exp[-(V - V_{1/2})/k])$, where G_{max} is the maximum conductance, $V_{1/2}$ is the potential at half-maximal conductance, and k is the slope of the activation curve. All data are expressed as mean ± s.e.m. and statistical analyses were performed using GraphPad Prism software (GraphPad, San Diego, CA, USA).

The apoptotic stimulus for electrophysiological experiments was a 10 min exposure to 30 μM 2,2-dithiodipyridine (DTDP) at 37 °C, 5% CO_2 (Aizenman *et al.*, 2000). The solution was aspirated and rat cortical cell cultures were thoroughly rinsed using 2 mL MHB (37° C) two times. Prior to electrophysiological experiments, rat cortical cell cultures were incubated for 3 hours in fresh medium containing 10 μM butoxy-carbonyl-aspartate-fluoromethyl ketone (BAF), a broad-spectrum protease inhibitor, limiting apoptosis subsequent to $K_V2.1$-mediated K^+ efflux (McLaughlin *et al.*, 2001).

Toxicity assays

Neuronal toxicity assays were conducted at 24 hours post transfection in luciferase co-transfected cells. Cells were thoroughly rinsed immediately before treatment with Minimal Essential Medium with Earle's salts (without phenol red) containing 0.01% bovine serum albumin and 25 mM HEPES. For one set of experiments, microglial cells (Cheepsunthorn et al., 2001) were plated directly onto cortical neurons and then activated by exposure to 10 U/mL interferon-γ and 1 μg/mL lipopolysaccharide for 60 min. Toxicity was assayed 24 hours later as described earlier (Knoch et al., 2008). In a separate set of experiments, cells were exposed to either DMSO vehicle (0.03%) or 30 μM 2,2′-dithiodipyridine (DTDP) for 10 min at 37°C, 5% CO_2. Toxicity was assayed 24 hours later. As an index of cell viability in transfected cells, luciferase activity (Boeckman & Aizenman, 1996; Rameau *et al.*, 2000; Aras *et al.*, 2008) was measured using the Steadylite Plus High Sensitivity Luminescence Reporter Gene Assay System (6066751, PerkinElmer Life Sciences, Boston, MA, USA) in a Victor2 Multilabel Counter (PerkinElmer Life Sciences).

Confocal imaging

For live imaging, neurons were transfected using Lipofectamine-2000 with plasmids expressing Tomato Red, eGFP-tagged $K_V2.1$ and either $K_V2.2$CT or $K_V2.1$C1a. Groups were compared to each corresponding empty vector, and imaged 48 hours later on a Nikon A1+ confocal microscope. For endogenous $K_V2.1$ antibody staining, neurons were first transfected with $K_V2.2$CT or corresponding vector, as well as with an eGFP-expressing plasmid. 48 hours later, cells were rinsed two times with 1× PBS, and fixed in 4% paraformaldehyde. After three washes with PBS, neurons were permeabilized for five minutes in PBS containing 0.3% Triton X-100. Neurons were then washed three times with PBS, incubated in PBS containing 1% bovine serum albumin for five minutes, and then incubated overnight with anti-$K_V2.1$ rabbit polyclonal antibody (Alomone Labs; 1:500). Cells were then washed five times with PBS, and after incubating for sixty minutes with AlexaFluor anti-rabbit 594 (Life Technologies; 1:1000), coverslips containing neurons were

mounted on glass slides and air-dried before imaging on a Nikon A1+ confocal microscope. For both live and fixed cell imaging, five–ten optical sections (0.5 μm) were acquired to generate a maximum intensity projection image that was analyzed for channel cluster counts and surface area using Nikon Instruments Elements Advanced Research software.

Immunoprecipitation and immunoblotting

CHO cells were used for both immunoprecipitation and immunoblot experiments. Briefly, cells were lysed in either Cell Extraction Buffer or NP40 Cell Lysis Buffer for immunoblotting and immunoprecipitation, respectively. Both lysis buffers were supplemented with phenylmethylsulfonyl fluoride and complete protease inhibitor cocktail tablet (Roche, Penzberg, Germany). Centrifugation, 10,000 × gravity for 10 minutes at 4°C, was used to remove cellular debris from samples. The protein concentrations were then measured using BCA protein assay kit (23225, Pierce, Thermo-Fisher, Pittsburgh, PA, USA). Protein samples were stored at −20°C until use.

For immunoprecipitation, equal amounts (0.7–1 mg) of protein were pre-cleared using 50 μl of resuspended volume of protein A/G plus-agarose (Santa Cruz, Dallas, TX, USA) for 1 hour at 4°C. Supernatants were then incubated, while gently agitating, with an antibody to syntaxin at 4°C for 3 hours with 90 μl of resuspended volume of beads. The samples were allowed to incubate overnight with gentle agitation. Protein-bound beads were then washed 3 times with PBS. Prior to loading onto 8% gels, equal amounts of total protein samples or beads were incubated with a 2× reducing sample buffer at 100°C for 5 min. Proteins were separated by sodium dodecyl sulfate-polyacrylamide gel (8%) electrophoresis using the Mini Protein 3 System (BioRad, Hercules, CA, USA) and transferred onto 0.2 μm nitrocellulose membranes. The membranes were then blocked at room temperature for one hour with 1% BSA in PBS containing 0.05% Tween 20 (PBST). The resultant blots were then incubated at room temperature for one hour with primary antibodies diluted in PBST with 1% BSA. Finally, after washing 3× in PBST, membranes were incubated with a Li-Cor IRDye-conjugated secondary antibody labeled with IRDye 800CW (780 nm), at 1:20,000, for 1 hour at RT. Fluorescent signals were acquired and quantified using the Odyssey Infrared Imaging System (LI-COR, Lincoln, NE, USA)

Plasmids and antibodies

The following plasmids were used in this study; eGFP (pCMVIE-eGFP; Clontech, Palo Alto, CA, USA), K_V2.1-eGFP (eGFP-C1; kind gift from D.P. Muhaptra), Tomato Red (pCSCMV;TdTomato #30530; Addgene, Cambridge, MA, USA), K_V2.2CT (pBK; kind gift from K.M. O'Connell), and K_V2.1C1a (pCDNA3; kind gift from I. Lotan). The following primary antibodies were used in this study; mouse anti-syntaxin from Millipore (Temecula, CA, USA), mouse anti-K_V2.1 from NeuroMab (Davis, CA, USA), mouse anti-β-actin from Sigma Aldrich (St. Louis, MO, USA), and rabbit anti- K_V2.1 (Alomone Labs, Jerusalem, Israel). The following mouse or rabbit secondary antibodies were used; Licor IRDye 800CW (LI-COR, Lincoln, NE, USA), Life Technologies anti-rabbit AlexaFluor 594 (Thermo-Fisher Scientific, Waltham, Massachusetts, USA).

Results

K_V2.2 CT mediates a calcineurin-independent dispersal of K_V2.1 somato-dendritic clusters

We first conducted an immuno-histochemical analysis of endogenous K_V2.1 somato-dendritic clusters as well as clusters produced in K_V2.1-eGFP expressing cortical neurons. The example confocal images of somato-dendritic clusters shown in Figure 1A & B, demonstrate that transfection with a plasmid encoding K_V2.2CT disrupted both endogenous (Figure 1A) as well as ectopically expressed K_V2.1-eGFP in rat cortical neurons (Figure 1B). Similar to observations in rat hippocampal neurons and HEK293 cells (Baver & O'Connell, 2012), expression of K_V2.2CT induced a greater than 2× fold decrease in clusters/area/cell (Figure 1C). Importantly, we found that treatment with the calcineurin inhibitor FK520 (5 μM), without ionomycin present, had no effect on K_V2.2CT-mediated K_V2.1 channel dispersal in neurons (Figure 1 B–C), indicating that K_V2.2CT causes dispersal of K_V2.1 somato-dendritic clusters without altering the activity of calcineurin.

Numerous stimuli induce dispersal of K_V2.1 somato-dendritic channel clusters, occurring concomitantly with hyperpolarized shifts in the $V_{1/2}$ of the channel (Misonou *et al.*, 2004; Misonou *et al.*, 2005a; Misonou *et al.*, 2006; Mohapatra & Trimmer, 2006; Mohapatra *et al.*, 2007; Mulholland *et al.*, 2008). This has been attributed to dephosphorylation of key amino acids, mainly located on the C-terminus of K_V2.1, by calcineurin, a calcium- and calmodulin-dependent serine/threonine protein phosphatase (Misonou *et al.*, 2004; Misonou *et al.*, 2005a; Misonou *et al.*, 2006; Park *et al.*, 2006; Park *et al.*, 2007; Mohapatra *et al.*, 2009). To determine whether co-expression of K_V2.2CT influences the phosphorylation state of K_V2.1, we first measured overall K_V2.1 phosphorylation status in vector- and K_V2.2CT-expressing CHO cells treated with ionomycin, a calcineurin-activating Ca^{2+} ionophore. Since CHO cells display a robust transfection efficiency compared to rat cortical neuronal cultures, they were used for this biochemical analysis. Western blots revealed that, K_V2.1 electrophoretic motility increased in CHO cells treated with ionomycin, indicating dephosphorylation of multiple channel residues. K_V2.2CT expression had no effect on basal or ionomycin-dependent electrophoretic motility (Figure 1D–E), suggesting that expression of this plasmid does not influence the phosphorylation status of K_V2.1. Combined, these results suggest that K_V2.2CT induced the disruption of K_V2.1 somato-dendritic clusters by a unique mechanism that is independent of channel dephosphorylation by calcineurin.

K_V2.2CT expression does not influence voltage-dependent activation of K_V2.1

In order to establish an unambiguous analysis of the effects of K_V2.1 channel localization, independent of function, we next confirmed that K_V2.2CT had no effect on steady-state voltage-dependent activation or current density in cortical neurons, as previously reported for other cell types (Baver & O'Connell, 2012). Comparison of neuronal delayed rectifier currents of non-transfected, pBK vector, and K_V2.2CT demonstrated that there was no effect on the steady-state voltage-dependent activation, $V_{1/2}$ (Figures 2A–B). Furthermore, our data demonstrated that, compared to non-transfected and pBK controls, the expression of K_V2.2CT had no effect on current density (Figure 2B). Combined with Figure 1, our data demonstrate that utilizing K_V2.2CT to induce dispersal of K_V2.1 somato-dendritic clusters, without altering the electrophysiological properties of the channel, is an acceptable model to

distinguish the putative neuroprotective effects of altering the localization of $K_V2.1$ from those induced by changing the activation profile of $K_V2.1$.

$K_V2.2CT$ expression decreases susceptibility to oxidative stress-inducing neuronal death

In order to establish whether $K_V2.2CT$ induced dispersal of $K_V2.1$ somato-dendritic clusters is associated with neuroprotection, we challenged cultured rat cortical neurons to oxidative apoptotic stimuli. DTDP (2,2′-dithio-bis-nitrobenzoic acid), a thiol-reactive oxidizing agent, was used to initiate a well characterized zinc- and calcium-dependent signaling cascade compulsory for *de novo* trafficking of the $K_V2.1$ channel to the plasma membrane and the induction of the apoptotic program (McCord & Aizenman, 2014). Twenty-four hours following a 10 minute exposure to 30 μM DTDP we observed widespread changes associated with cell death in cortical neurons previously transfected with a tomato red-expressing plasmid (Figure 3A). Expression of $K_V2.2CT$, effectively protected neurons from this apoptotic stimulus and precluded any identifiable morphological changes typical of apoptosis (Figure 3A). Moreover, $K_V2.2CT$ increased neuronal viability following DTDP treatment compared to control, when quantified using a luciferase viability assay (Figure 3B). $K_V2.2CT$ expression was also protective when utilizing a more pathophysiologically-relevant injurious stimulus, activated microglia (Figure 3B), which we have reported to proceed via the same zinc-activated and $K_V2.1$ current-dependent cell signaling pathway (Knoch *et al.*, 2008). These findings support our hypothesis and suggest that $K_V2.1$ somato-dendritic clusters may serve a vital role in regulating apoptotic trafficking of $K_V2.1$ channels in response to oxidative stress-induced neuronal death.

We next evaluated whether $K_V2.1$ clusters remained intact following DTDP exposure. DTDP induces Zn^{2+} liberation from intracellular stores (Aizenman et al., 2000), which, in turn can mediate Ca^{2+} release via ryanodine receptors (Woodier et al., 2015; Schulien et al., 2016). As such, Zn^{2+}, under certain circumstances, may induce calcineurin-dependent $K_V2.1$ declustering (Schulien et al., 2016). Interestingly, $K_V2.1$ clusters remained intact following a brief 10 minute treatment with 30 μM DTDP, at least for approximately 90 minutes following exposure (Figure 3C). This is consistent with the fact that DTDP is an effective stimulus for the delayed apoptogenic insertion of $K_V2.1$ channels (McLaughlin et al., 2001), as clusters remain stable for a surprisingly long period following the exposure to the oxidant. A pronounced redistribution of channels was indeed observed and measured 3–4.5 hours after the DTDP exposure, which was completely prevented by the addition of the Zn^{2+} chelator N,N,N′,N′-Tetrakis(2-pyridylmethyl)ethylenediamine (TPEN; 10 μM), consistent with the aforementioned observations on the role of the metal in $K_V2.1$ declustering (Figure 3D). Our evidence, however, suggests that clusters remain stable following DTDP exposure for a sufficient amount of time to allow apoptotic trafficking.

$K_V2.2CT$ expression blocks pro-apoptotic K^+ currents

In order to determine whether $K_V2.1$ somato-dendritic clusters are critical for apoptogenic $K_V2.1$ trafficking and the consequent $K_V2.1$-mediated efflux, we conducted a set of whole cell voltage-clamp experiments using a lethal dose of DTDP. Whole cell voltage-clamp experiments conducted 3–4.5 hours after a 10 minute exposure to DTDP (30 μM) revealed that increased $K_V2.1$ mediated current density observed in pBK vector-expressing cortical

neuron controls was absent in cells over-expressing K_V2.2CT (Figure 3E). Thus, expressing K_V2.2CT, which induces dispersal of K_V2.1 channel clusters (Baver & O'Connell, 2012) without altering electrophysiological properties of the channel, eliminated the pro-apoptotic K^+ current density increase, and reduced susceptibility to oxidative-stress induced neuronal death in DTDP-treated neurons.

K_V2.2CT acts through a distinct mechanism that differs from K_V2.1C1a

We previously reported that expression of K_V2.1C1a (rat K_V2.1 A.A. 441–522) alone confers protection against oxidative stress by preventing K_V2.1 from binding to syntaxin, thereby abrogating apoptogenic increases in K_V2.1 mediated currents (McCord *et al.*, 2014). K_V2.1 and K_V2.2 isoforms have been demonstrated to interact with syntaxin 1a. Although the syntaxin binding domain of K_V2.1 has been determined, the precise domain(s) responsible for this remain(s) undefined for the K_V2.2 isoform (Michaelevski *et al.*, 2003; Wolf-Goldberg *et al.*, 2006). Since both K_V2.2CT and K_V2.1C1a seem to block trafficking of K_V2.1 in response to lethal stimuli, we next conducted experiments to differentiate these two K_V2 channel derived neuroprotective agents.

First, we investigated whether K_V2.1C1a could disperse K_V2.1 somato-dendritic clusters and found that, in contrast to K_V2.2CT, expression of K_V2.1C1a had no effect on somato-dendritic clusters compared to control (Figure 1A–B, Figure 4A–B). Next, we evaluated whether K_V2.2CT could prevent the association of K_V2.1 with syntaxin. In contrast to K_V2.1C1a (McCord *et al.*, 2014), K_V2.2CT did not cause a decrease in the association of K_V2.1 with syntaxin 1A (Figure 4C). Therefore, these two K_V2 channel-derived neuroprotective proteins work through a unique mechanism, despite the finding that both block the downstream step of K^+ efflux. As such, K_V2.1 somato-dendritic clusters appear to serve a vital role in oxidative stress-induced apoptogenic trafficking of K_V2.1. Based on our findings, K_V2.2CT provides a potentially useful pharmacotherapeutic model to limit neuronal cell death in response to oxidative stress.

Discussion

In this study, we evaluated the role of K_V2.1 somato-dendritic clusters in oxidative stress-induced neuronal death. Specifically, we hypothesized that the dispersal of these structures would increase neuronal viability following lethal oxidative stress exposure by prohibiting the increase in K^+ efflux mediated by K_V2.1 channels, which we have previously demonstrated to be due to insertion of new channels into the plasma membrane (Pal *et al.*, 2006). Oxidants can initiate a highly characterized neuronal cell death pathway that involves Zn^{2+}- and Ca^{2+}-dependent enzymatic events, culminating on the phosphorylation of key residues located on the N- and C-termini of K_V2.1, Y124 and S800 by Src and p38, respectively (McCord & Aizenman, 2013; He *et al.*, 2015). These post-translational processes result in an increased association of syntaxin with the C1a region of K_V2.1, thereby permitting *de novo* trafficking of the channel and potassium efflux required for the induction and maintenance of the apoptotic cell death program (Pal *et al.*, 2006; McCord *et al.*, 2014). Importantly, blocking apoptogenic trafficking of K_V2.1 significantly improved neuronal viability (Pal *et al.*, 2003; Pal *et al.*, 2006; Shepherd *et al.*, 2012; McCord &

Aizenman, 2013; Shepherd *et al.*, 2013; McCord *et al.*, 2014). Our data suggest that the dispersal of $K_V2.1$ clusters by $K_V2.2$CT not only blocks apoptogenic K^+ currents, but is also sufficient for providing neuroprotection.

$K_V2.2$CT contains a homologous domain responsible for the restricted and polarized localization of K_V2 channels, known as the proximal restriction and clustering domain (PRC) (Lim *et al.*, 2000). Our data confirm that expression of $K_V2.2$CT induced a dispersal of $K_V2.1$ somato-dendritic clusters in cortical neurons without altering basal current density, voltage-dependent steady-state activation, basal phosphorylation state as well as calcium-dependent dephosphorylation, and importantly did not require calcineurin activity, an important component of other $K_V2.1$ cluster dispersal processes induced by a number of physiological and injurious stimuli (Misonou et al., 2004; Mulholland et al., 2008; Aras et al., 2009a; Baver and O'Connell, 2012; Shepherd et al., 2012; Shah and Aizenman, 2014).

Unlike $K_V2.1$C1a, the proximal region of the C-terminal known to interact with syntaxin (Singer-Lahat et al., 2007; McCord et al., 2014), co-immunoprecipitation experiments demonstrated that $K_V2.2$CT does not displace the interaction of $K_V2.1$ with the SNARE protein. The $K_V2.1$C1a protein used in this study is derived from amino acids 441–522 of the C-terminus of $K_V2.1$ (McCord *et al.*, 2014), and lacks the PRC domain essential for localization of $K_V2.1$ to somato-dendritic clusters (Lim *et al.*, 2000). Demonstrative of this fact, over-expression of $K_V2.1$C1a had no effect on the localization of $K_V2.1$ to somato-dendritic clusters. This result is in accordance with a previous study in which a $K_V2.1$-mutant lacking the syntaxin binding domain also failed to disrupt $K_V2.1$ somato-dendritic clusters (Fox *et al.*, 2015). This is in contrast to $K_V2.2$CT, which contains a PRC domain sharing approximately 65% homology with $K_V2.1$ (rat $K_V2.1$ A.A. 572–598; rat $K_V2.2$ A.A. 592–617) and does cause the dispersal of $K_V2.1$ somato-dendritic clusters, suggesting that C-terminal domains other than C1a also contribute to the regulation of apoptogenic trafficking of $K_V2.1$.

The precise time point at which new channels are inserted following an apoptotic stimulus is not known. Given the observable disruption of $K_V2.1$ somato-dendritic clusters by DTDP after 90 minutes, at least under our current experimental conditions (i.e. transfected channels), apoptogenic trafficking may occur relatively early in the process. Since only a small fraction of the total number of $K_V2.1$ channels expressed on the plasma membrane at any given time are functionally active (Fox et al. 2013), an unknown silencing mechanism may exist, even in the newly inserted channels, which slowly dissipates over time. This exciting proposition will be the subject of a future study. In any event, although significantly declustered by 3–4.5 hours post DTDP, $K_V2.1$ clusters are remarkably resilient to oxidant exposure, providing the physical scaffolding sites necessary for apoptogenic trafficking.

In response to sub lethal stimuli, including ischemia, endogenous neuroprotective pathways are activated, which allow neurons to effectively avert the consequences of subsequent challenges that would otherwise be lethal (Kitagawa *et al.*, 1990; Gidday, 2006; Aras *et al.*, 2009b). In neurons, this process termed preconditioning, relies on a transient increase in free Zn^{2+} and activation of the Ca^{2+}-dependent phosphatase calcineurin (Lockshin & Williams, 1965; Aras *et al.*, 2009b; Schulien *et al.*, 2016). Our laboratory previously reported that,

preconditioned neurons display dispersed $K_V2.1$ somato-dendritic clusters (Aras *et al.*, 2009b). It is thus entirely possible that changes in $K_V2.1$ localization in preconditioned neurons are responsible, at least in part, for resistance to subsequent, normally lethal stimuli. As such, elucidation of the processes regulating $K_V2.1$ channel localization may reveal intrinsic neuro-adaptive mechanisms potentially representing unique pharmacotherapeutic targets. Transient dispersal of $K_V2.1$ somato-dendritic clusters may prove to be an effective mechanism limiting neuronal cell loss in response to a variety of acute and progressive neurodegenerative conditions in which oxidative stress is known to play a key role

Acknowledgments

We thank D.P. Mohapatra, Washington University, St. Louis, for GFP-$K_V2.1$-expressing plasmid. We also thank K.M. O'Connell, University of Tennessee Health Science Center, for $K_V2.2$CT-expressing plasmid. Finally, we thank I. Lotan, Tel Aviv University, for the $K_V2.1$C1a plasmid. This work was supported by NIH grant NS043277 to E.A. N.H.S. was supported by the American Heart Association Pre-doctoral Fellowship 12PRE11070001. J.A.J. was supported by NIH T32 NS086749. All authors have contributed to research and article preparation. All authors have approved the final version of this manuscript and declare no competing interests.

Abbreviations

$K_V2.2$CT	protein derived from the c-terminus of $K_V2.2$
$K_V2.1$C1a	protein derived from $K_V2.1$ c-terminus (syntaxin binding domain)
DTDP	2,2′-dithiodipyridine
eGFP	enhanced green fluorescent protein
CHO	Chinese hamster ovary
PBS	phosphate buffered saline
DMSO	dimethyl sulfoxide
K_V	voltage dependent potassium channel
$V_{1/2}$	voltage of steady-state half-maximal activation
PRC	proximal restriction and clustering domain

References

Aizenman E, Stout AK, Hartnett KA, Dineley KE, McLaughlin B, Reynolds IJ. Induction of neuronal apoptosis by thiol oxidation: putative role of intracellular zinc release. J Neurochem. 2000; 75:1878–1888. [PubMed: 11032877]

Aras MA, Hara H, Hartnett KA, Kandler K, Aizenman E. Protein kinase C regulation of neuronal zinc signaling mediates survival during preconditioning. J Neurochem. 2009a; 110:106–117. [PubMed: 19453299]

Aras MA, Hartnett KA, Aizenman E. Assessment of cell viability in primary neuronal cultures. Curr Protoc Neurosci. 2008:18. Chapter 7, Unit 7. [PubMed: 18633999]

Aras MA, Saadi RA, Aizenman E. Zn2+ regulates Kv2.1 voltage-dependent gating and localization following ischemia. Eur J Neurosci. 2009b; 30:2250–2257. [PubMed: 20092568]

Baver SB, O'Connell KM. The C-terminus of neuronal Kv2.1 channels is required for channel localization and targeting but not for NMDA-receptor-mediated regulation of channel function. Neuroscience. 2012; 217:56–66. [PubMed: 22554782]

Boeckman FA, Aizenman E. Pharmacological properties of acquired excitotoxicity in Chinese hamster ovary cells transfected with N-methyl-D-aspartate receptor subunits. J Pharmacol Exp Ther. 1996; 279:515–523. [PubMed: 8930153]

Bortner CD, Cidlowski JA. Cell shrinkage and monovalent cation fluxes: role in apoptosis. Arch Biochem Biophys. 2007; 462:176–188. [PubMed: 17321483]

Bortner CD, Hughes FM Jr, Cidlowski JA. A primary role for K+ and Na+ efflux in the activation of apoptosis. J Biol Chem. 1997; 272:32436–32442. [PubMed: 9405453]

Cheepsunthorn P, Radov L, Menzies S, Reid J, Connor JR. Characterization of a novel brain-derived microglial cell line isolated from neonatal rat brain. Glia. 2001; 35:53–62. [PubMed: 11424192]

Cobb MM, Austin DC, Sack JT, Trimmer JS. Cell Cycle-dependent Changes in Localization and Phosphorylation of the Plasma Membrane Kv2.1 K+ Channel Impact Endoplasmic Reticulum Membrane Contact Sites in COS-1 Cells. J Biol Chem. 2015; 290:29189–29201. [PubMed: 26442584]

Danial NN, Korsmeyer SJ. Cell death: critical control points. Cell. 2004; 116:205–219. [PubMed: 14744432]

Du J, Haak LL, Phillips-Tansey E, Russell JT, McBain CJ. Frequency-dependent regulation of rat hippocampal somato-dendritic excitability by the K+ channel subunit Kv2.1. J Physiol. 2000; 522(Pt 1):19–31. [PubMed: 10618149]

Fox PD, Haberkorn CJ, Akin EJ, Seel PJ, Krapf D, Tamkun MM. Induction of stable ER-plasma-membrane junctions by Kv2.1 potassium channels. J Cell Sci. 2015; 128:2096–2105. [PubMed: 25908859]

Fox PD, Haberkorn CJ, Weigel AV, Higgins JL, Akin EJ, Kennedy MJ, Krapf D, Tamkun MM. Plasma membrane domains enriched in cortical endoplasmic reticulum function as membrane protein trafficking hubs. Mol Biol Cell. 2013; 24:2703–2713. [PubMed: 23864710]

Gidday JM. Cerebral preconditioning and ischaemic tolerance. Nat Rev Neurosci. 2006; 7:437–448. [PubMed: 16715053]

Guan D, Armstrong WE, Foehring RC. Kv2 channels regulate firing rate in pyramidal neurons from rat sensorimotor cortex. J Physiol. 2013; 591:4807–4825. [PubMed: 23878373]

Hartnett KA, Stout AK, Rajdev S, Rosenberg PA, Reynolds IJ, Aizenman E. NMDA receptor-mediated neurotoxicity: a paradoxical requirement for extracellular Mg2+ in Na+/Ca2+-free solutions in rat cortical neurons in vitro. J Neurochem. 1997; 68:1836–1845. [PubMed: 9109508]

He K, McCord MC, Hartnett KA, Aizenman E. Regulation of Pro-Apoptotic Phosphorylation of Kv2.1 K+ Channels. PLoS One. 2015; 10:e0129498. [PubMed: 26115091]

Huang H, Gao TM, Gong L, Zhuang Z, Li X. Potassium channel blocker TEA prevents CA1 hippocampal injury following transient forebrain ischemia in adult rats. Neurosci Lett. 2001; 305:83–86. [PubMed: 11376889]

Hughes FM Jr, Bortner CD, Purdy GD, Cidlowski JA. Intracellular K+ suppresses the activation of apoptosis in lymphocytes. J Biol Chem. 1997; 272:30567–30576. [PubMed: 9374553]

Hughes FM Jr, Cidlowski JA. Potassium is a critical regulator of apoptotic enzymes in vitro and in vivo. Adv Enzyme Regul. 1999; 39:157–171. [PubMed: 10470372]

Kitagawa K, Matsumoto M, Tagaya M, Hata R, Ueda H, Niinobe M, Handa N, Fukunaga R, Kimura K, Mikoshiba K, et al. 'Ischemic tolerance' phenomenon found in the brain. Brain Res. 1990; 528:21–24. [PubMed: 2245337]

Knoch ME, Hartnett KA, Hara H, Kandler K, Aizenman E. Microglia induce neurotoxicity via intraneuronal Zn(2+) release and a K(+) current surge. Glia. 2008; 56:89–96. [PubMed: 17955552]

Li J, Baud O, Vartanian T, Volpe JJ, Rosenberg PA. Peroxynitrite generated by inducible nitric oxide synthase and NADPH oxidase mediates microglial toxicity to oligodendrocytes. Proc Natl Acad Sc USA. 2005; 102:9936–9941. [PubMed: 15998743]

Lim ST, Antonucci DE, Scannevin RH, Trimmer JS. A novel targeting signal for proximal clustering of the Kv2.1 K+ channel in hippocampal neurons. Neuron. 2000; 25:385–397. [PubMed: 10719893]

Lockshin RA, Williams CM. Programmed cell death. IV. The influence of drugs on the breakdown of the intersegmental muscles of silkmoths. J Insect Physiol. 1965; 11:803–809. [PubMed: 5827539]

Malin SA, Nerbonne JM. Delayed rectifier K+ currents, IK, are encoded by Kv2 alpha-subunits and regulate tonic firing in mammalian sympathetic neurons. J Neurosci. 2002; 22:10094–10105. [PubMed: 12451110]

McCord MC, Aizenman E. Convergent Ca2+ and Zn2+ signaling regulates apoptotic Kv2.1 K+ currents. Proc Natl Acad Sci U S A. 2013; 110:13988–13993. [PubMed: 23918396]

McCord MC, Aizenman E. The role of intracellular zinc release in aging, oxidative stress, and Alzheimer's disease. Front Aging Neurosci. 2014; 6:77. [PubMed: 24860495]

McCord MC, Kullmann PH, He K, Hartnett KA, Horn JP, Lotan I, Aizenman E. Syntaxin-binding domain of Kv2.1 is essential for the expression of apoptotic K+ currents. J Physiol. 2014; 592:3511–3521. [PubMed: 24928958]

McLaughlin B, Pal S, Tran MP, Parsons AA, Barone FC, Erhardt JA, Aizenman E. p38 activation is required upstream of potassium current enhancement and caspase cleavage in thiol oxidant-induced neuronal apoptosis. J Neurosci. 2001; 21:3303–3311. [PubMed: 11331359]

Michaelevski I, Chikvashvili D, Tsuk S, Singer-Lahat D, Kang Y, Linial M, Gaisano HY, Fili O, Lotan I. Direct interaction of target SNAREs with the Kv2.1 channel. Modal regulation of channel activation and inactivation gating. J Biol Chem. 2003; 278:34320–34330. [PubMed: 12807875]

Misonou H, Menegola M, Mohapatra DP, Guy LK, Park KS, Trimmer JS. Bidirectional activity-dependent regulation of neuronal ion channel phosphorylation. J Neurosci. 2006; 26:13505–13514. [PubMed: 17192433]

Misonou H, Mohapatra DP, Menegola M, Trimmer JS. Calcium- and metabolic state-dependent modulation of the voltage-dependent Kv2.1 channel regulates neuronal excitability in response to ischemia. J Neurosci. 2005a; 25:11184–11193. [PubMed: 16319318]

Misonou H, Mohapatra DP, Park EW, Leung V, Zhen D, Misonou K, Anderson AE, Trimmer JS. Regulation of ion channel localization and phosphorylation by neuronal activity. Nat Neurosci. 2004; 7:711–718. [PubMed: 15195093]

Misonou H, Mohapatra DP, Trimmer JS. Kv2.1: a voltage-gated k+ channel critical to dynamic control of neuronal excitability. Neurotoxicology. 2005b; 26:743–752. [PubMed: 15950285]

Mohapatra DP, Misonou H, Pan SJ, Held JE, Surmeier DJ, Trimmer JS. Regulation of intrinsic excitability in hippocampal neurons by activity-dependent modulation of the KV2.1 potassium channel. Channels (Austin). 2009; 3:46–56. [PubMed: 19276663]

Mohapatra DP, Park KS, Trimmer JS. Dynamic regulation of the voltage-gated Kv2.1 potassium channel by multisite phosphorylation. Biochem Soc Trans. 2007; 35:1064–1068. [PubMed: 17956280]

Mohapatra DP, Trimmer JS. The Kv2.1 C terminus can autonomously transfer Kv2.1-like phosphorylation-dependent localization, voltage-dependent gating, and muscarinic modulation to diverse Kv channels. J Neurosci. 2006; 26:685–695. [PubMed: 16407566]

Montague JW, Bortner CD, Hughes FM Jr, Cidlowski JA. A necessary role for reduced intracellular potassium during the DNA degradation phase of apoptosis. Steroids. 1999; 64:563–569. [PubMed: 10503710]

Mulholland PJ, Carpenter-Hyland EP, Hearing MC, Becker HC, Woodward JJ, Chandler LJ. Glutamate transporters regulate extrasynaptic NMDA receptor modulation of Kv2.1 potassium channels. J Neurosci. 2008; 28:8801–8809. [PubMed: 18753382]

Murakoshi H, Trimmer JS. Identification of the Kv2.1 K+ channel as a major component of the delayed rectifier K+ current in rat hippocampal neurons. J Neurosci. 1999; 19:1728–1735. [PubMed: 10024359]

Norris CA, He K, Springer MG, Hartnett KA, Horn JP, Aizenman E. Regulation of neuronal proapoptotic potassium currents by the hepatitis C virus nonstructural protein 5A. J Neurosci. 2012; 32:8865–8870. [PubMed: 22745487]

O'Connell KM, Loftus R, Tamkun MM. Localization-dependent activity of the Kv2.1 delayed-rectifier K+ channel. Proc Natl Acad Sci U S A. 2010; 107:12351–12356. [PubMed: 20566856]

O'Connell KM, Rolig AS, Whitesell JD, Tamkun MM. Kv2.1 potassium channels are retained within dynamic cell surface microdomains that are defined by a perimeter fence. J Neurosci. 2006; 26:9609–9618. [PubMed: 16988031]

Ohki EC, Tilkins ML, Ciccarone VC, Price PJ. Improving the transfection efficiency of post-mitotic neurons. J Neurosci Methods. 2001; 112:95–99. [PubMed: 11716945]

Pal S, Hartnett KA, Nerbonne JM, Levitan ES, Aizenman E. Mediation of neuronal apoptosis by Kv2.1-encoded potassium channels. J Neurosci. 2003; 23:4798–4802. [PubMed: 12832499]

Pal SK, Takimoto K, Aizenman E, Levitan ES. Apoptotic surface delivery of K+ channels. Cell Death Differ. 2006; 13:661–667. [PubMed: 16273079]

Park KS, Mohapatra DP, Misonou H, Trimmer JS. Graded regulation of the Kv2.1 potassium channel by variable phosphorylation. Science. 2006; 313:976–979. [PubMed: 16917065]

Park KS, Mohapatra DP, Trimmer JS. Proteomic analyses of K(v)2.1 channel phosphorylation sites determining cell background specific differences in function. Channels (Austin). 2007; 1:59–61. [PubMed: 18690023]

Rameau GA, Akaneya Y, Chiu L, Ziff EB. Role of NMDA receptor functional domains in excitatory cell death. Neuropharmacology. 2000; 39:2255–2266. [PubMed: 10974309]

Redman PT, Hartnett KA, Aras MA, Levitan ES, Aizenman E. Regulation of apoptotic potassium currents by coordinated zinc-dependent signalling. J Physiol. 2009; 587:4393–4404. [PubMed: 19622611]

Redman PT, He K, Hartnett KA, Jefferson BS, Hu L, Rosenberg PA, Levitan ES, Aizenman E. Apoptotic surge of potassium currents is mediated by p38 phosphorylation of Kv2.1. Proc Natl Acad Sci U S A. 2007; 104:3568–3573. [PubMed: 17360683]

Redman PT, Jefferson BS, Ziegler CB, Mortensen OV, Torres GE, Levitan ES, Aizenman E. A vital role for voltage-dependent potassium channels in dopamine transporter-mediated 6-hydroxydopamine neurotoxicity. Neuroscience. 2006; 143:1–6. [PubMed: 17027171]

Schulien AJ, Justice JA, Di Maio R, Wills ZP, Shah NH, Aizenman E. Zn(2+) -induced Ca(2+) release via ryanodine receptors triggers calcineurin-dependent redistribution of cortical neuronal Kv2.1 K(+) channels. J Physiol. 2016; 594:2647–2659. [PubMed: 26939666]

Shah NH, Aizenman E. Voltage-gated potassium channels at the crossroads of neuronal function, ischemic tolerance, and neurodegeneration. Transl Stroke Res. 2014; 5(1):38–58. [PubMed: 24323720]

Shen QJ, Zhao YM, Cao DX, Wang XL. Contribution of Kv channel subunits to glutamate-induced apoptosis in cultured rat hippocampal neurons. J Neurosci Res. 2009; 87:3153–3160. [PubMed: 19472219]

Shepherd AJ, Loo L, Gupte RP, Mickle AD, Mohapatra DP. Distinct modifications in Kv2.1 channel via chemokine receptor CXCR4 regulate neuronal survival-death dynamics. J Neurosci. 2012; 32:17725–17739. [PubMed: 23223293]

Shepherd AJ, Loo L, Mohapatra DP. Chemokine co-receptor CCR5/CXCR4-dependent modulation of Kv2.1 channel confers acute neuroprotection to HIV-1 glycoprotein gp120 exposure. PLoS One. 2013; 8:e76698. [PubMed: 24086760]

Singer-Lahat D, Sheinin A, Chikvashvili D, Tsuk S, Greitzer D, Friedrich R, Feinshreiber L, Ashery U, Benveniste M, Levitan ES, Lotan I. K+ channel facilitation of exocytosis by dynamic interaction with syntaxin. J Neurosc. 2007; 27(7):1651–1658.

Wei L, Xiao AY, Jin C, Yang A, Lu ZY, Yu SP. Effects of chloride and potassium channel blockers on apoptotic cell shrinkage and apoptosis in cortical neurons. Pflugers Arch. 2004; 448:325–334. [PubMed: 15057559]

Wolf-Goldberg T, Michaelevski I, Sheu L, Gaisano HY, Chikvashvili D, Lotan I. Target soluble N-ethylmaleimide-sensitive factor attachment protein receptors (t-SNAREs) differently regulate activation and inactivation gating of Kv2.2 and Kv2.1: Implications on pancreatic islet cell Kv channels. Mol Pharmacol. 2006; 70:818–828. [PubMed: 16754785]

Woodier J, Rainbow RD, Stewart AJ, Pitt SJ. Intracellular zinc modulates cardiac tyanodine receptor-mediated calcium release. J Biol Chem. 2015; 290(28):17599–17610. [PubMed: 26041778]

Yu SP, Yeh CH, Sensi SL, Gwag BJ, Canzoniero LM, Farhangrazi ZS, Ying HS, Tian M, Dugan LL, Choi DW. Mediation of neuronal apoptosis by enhancement of outward potassium current. Science. 1997; 278:114–117. [PubMed: 9311914]

Highlights

- K_V2.2CT induces dispersal of K_V2.1 somato-dendritic clusters independent of calcineurin-mediated dephosphorylation.
- K_V2.2CT decreases neuronal susceptibility to oxidative-stress induced death.
- K_V2.2CT abrogates the apoptogenic increases in K_V2.1-mediated currents.
- K_V2.1 somato-dendritic clusters may serve as physical scaffolding sites or signalosomes required for apoptotic trafficking of K_V2.1.

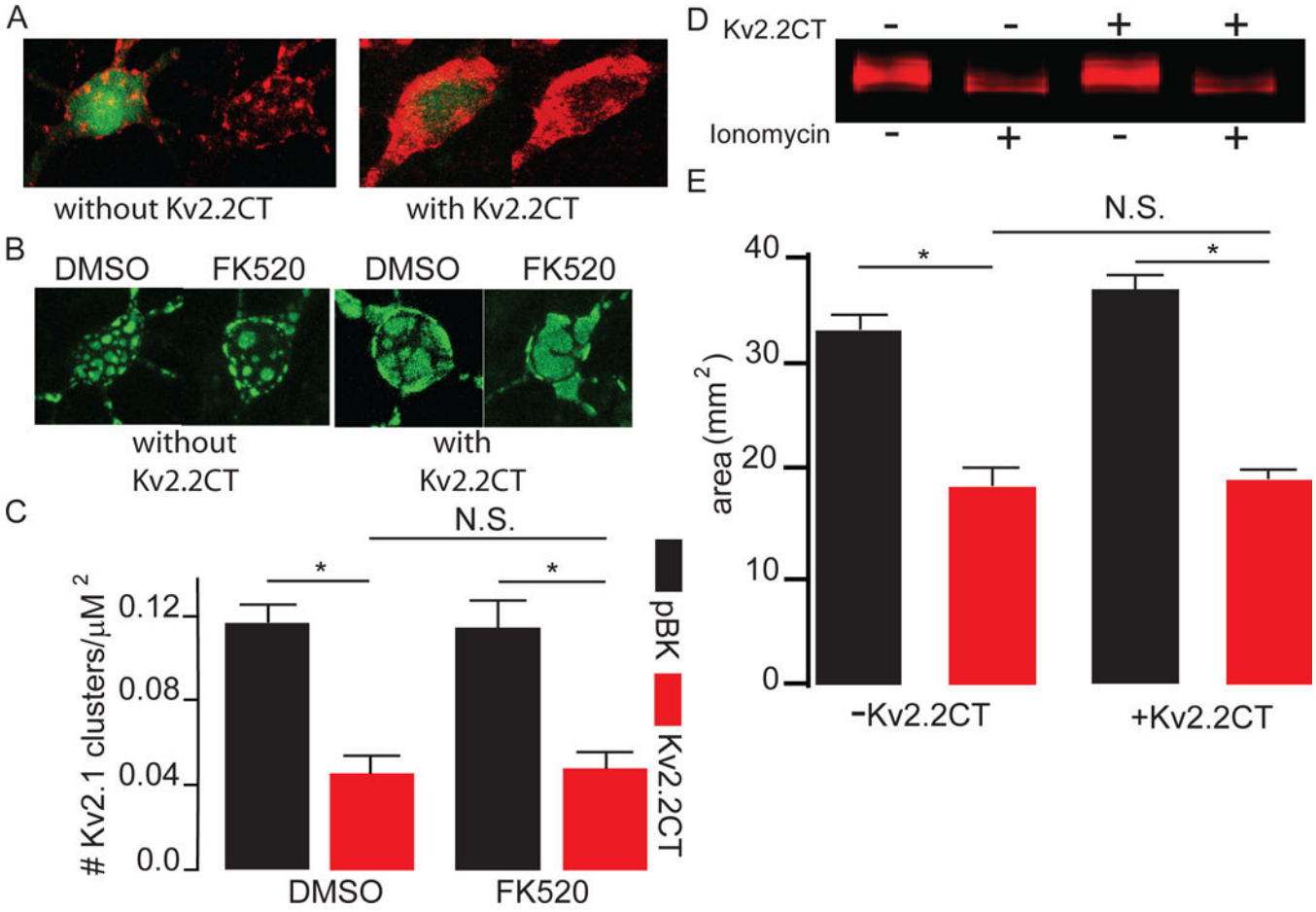

Figure 1. K_V2.2CT mediates a calcineurin independent dispersal of K_V2.1 somato-dendritic clusters

A) Example confocal images of cortical neurons demonstrating a significant disruption of endogenous K_V2.1 somato-dendritic clusters labelled with Alexafluor-594 2° Antibody with either eGFP plus pBK-vector (left two images), or eGFP plus K_V2.2CT (right two images). K_V2.2CT expression significantly disrupted the number of K_V2.1 somato-dendritic clusters/cell (without K_V2.2CT (pBK) 21±3.5 clusters/cell, n=12; with K_V2.2CT 11.1±2.1 clusters/cell, n=11; 2 tailed t-test, P=0.03. B) Example confocal images of neurons expressing K_V2.1-eGFP without K_V2.2CT (left two images) and neurons expressing K_V2.2CT and K_V2.1-eGFP (right two images). Cells were either treated with 0.01% DMSO or 5 μM FK520. C) Bar graph summary of data demonstrating that K_V2.2CT induces dispersal of K_V2.1 somato-dendritic clusters, independent of calcineurin activation (pBK/K_V2.1-eGFP + 0.01% DMSO 0.12 ± 0.01 clusters/μm^2, n=12; pBK/K_V2.1-eGFP + FK520 0.11 ± 0.01 clusters/μm^2, n= 13; K_V2.2CT/K_V2.1-eGFP + 0.01% DMSO 0.05 ± 0.01 clusters/μm^2, n=15; K_V2.2CT/K_V2.1-eGFP + FK520 0.048 ± 0.01 clusters/μm^2, n=18; one-way ANOVA and Bonferroni post-hoc test, P<0.0001). D) Example Western blot image of IRdye 800-labelled K_V2.1 comparing Ca^{2+} mediated dephosphorylation between pBK-vector (top minus symbols) and K_V2.2CT (top plus symbols) expressing CHO cells with ionomycin treatment (bottom plus symbols) or 0.01% DMSO (bottom minus symbols). E) Bar graph summary demonstrating that K_V2.2CT had no effect on the ability of ionomycin to cause

bulk dephosphorylation of the channel as measured by the area of the $K_V2.1$ band. (n=3 each; 33.01±1.5 mm^2 without $K_V2.2CT$; 18.5±1.7 mm^2 without $K_V2.2CT$ plus ionomycin; 36.7±1.3 mm^2 with $K_V2.2CT$; 19.1±1.0 mm^2 with $K_V2.2CT$ plus ionomyin; ANOVA and Tukey-Kramer post-hoc test, $P<0.0001$.

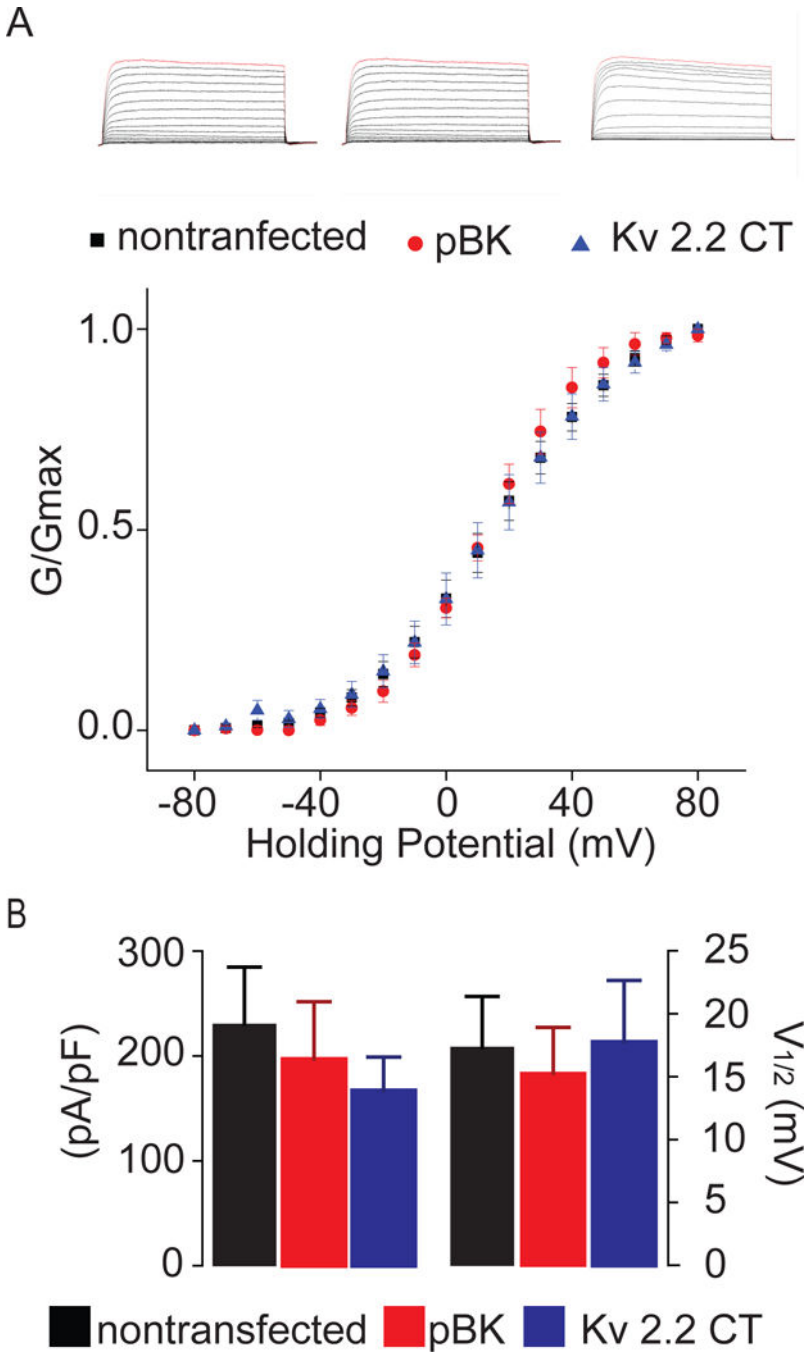

Figure 2. K_V2.2CT induces dispersal of K_V2.1 somato-dendritic clusters without altering the electrophysiological properties of the channel

A) (Top) From left to right, example whole-cell voltage-clamp current traces of non-transfected neurons, neurons expressing pBK vector alone, and neurons expressing K_V2.2CT, respectively. (Bottom) Summarized scatter plot of the voltage-dependent conductance (G-V) of non-transfected (black square), pBK vector alone (red circle), and K_V2.2CT (blue triangle). B) Summarized bar graphs of both current density, and voltage of half-maximal activation, $V_{1/2}$. Compared to non-transfected (230.47 ± 54.51 pA/pF; n=13) and pBK vector alone (194.25 ± 54.82 pA/pF; n=7), K_V2.2CT (167.25 ± 44.57 pA/pF;

n=10) had no significant effect on the current density of the delayed rectifier current (ANOVA, P= 0.66). Finally, we found that compared to non-transfected (19.81 ± 3.46 mV; n=13) and pBK vector alone (15.26 ± 3.66; n=7), K_V2.2CT (17.76 ± 4.9; n=10) had no significant effect on the steady-state voltage-dependent activation of the delayed rectifier current (ANOVA, P=0.9325).

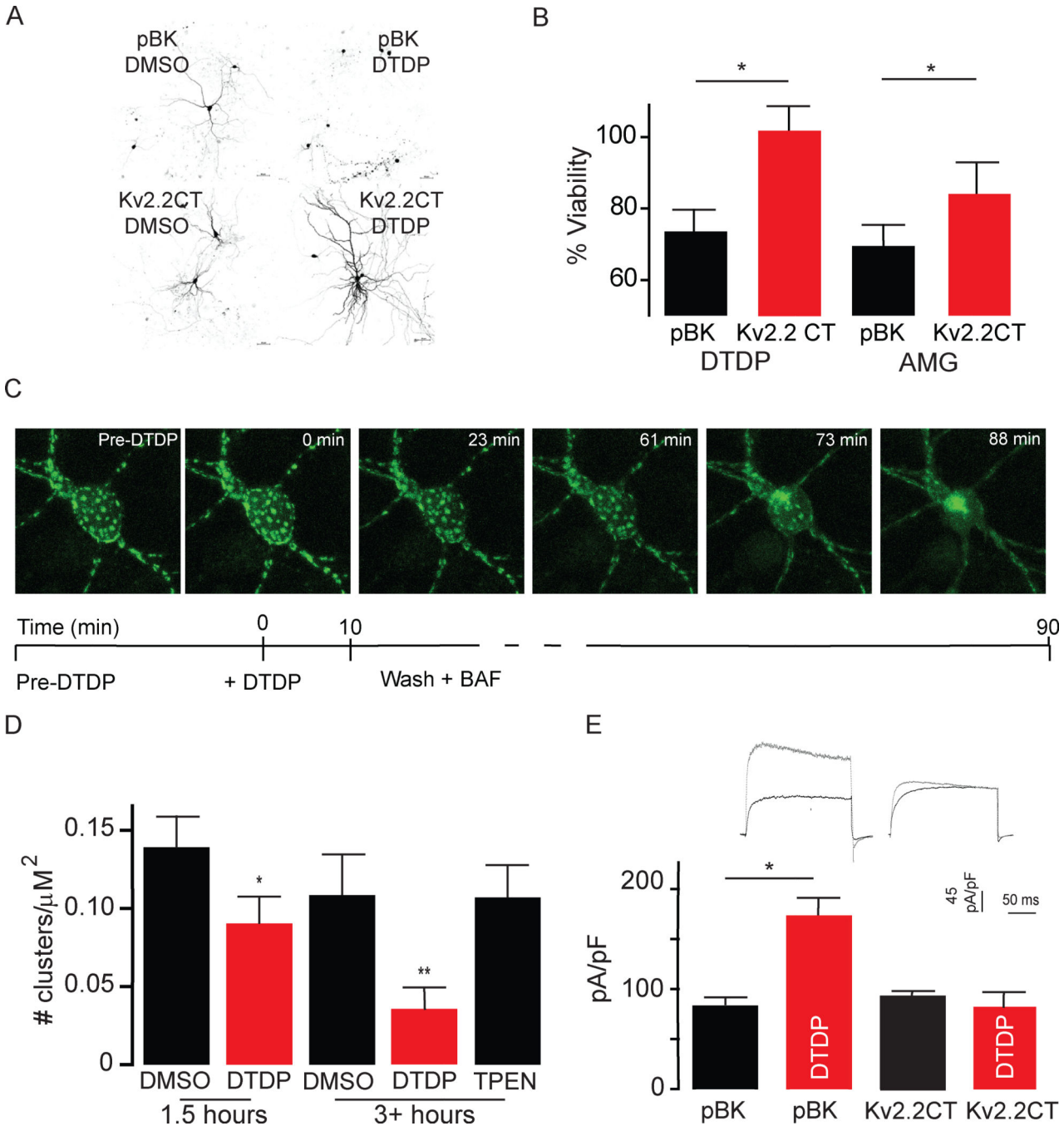

Figure 3. K^+_V2.2CT expression blocks proapoptotic K^+ currents and decreases neuronal susceptibility to oxidative stress-inducing apoptosis

A) Example confocal images of rat primary cortical neurons transfected with tomato-red and treated with either 0.01% DMSO or 30 μM DTDP for 10 minutes at 25 °C. Notably, K_V2.2CT expression improved neuronal viability compared to expression of vector-alone (pBK) as the apoptotic volume decrease, membrane blebbing and fragmentation of the dendritic arbor (top right) were no longer evident (bottom right). B) Bar graph summary of both a luciferase cell viability assay against 30 μM DTDP and activated microglia assay demonstrating that the expression of K_V2.2CT improves neuronal viability against both

forms of oxidative stress-induced apoptosis. Utilizing a 30 μM DTDP treatment for 10 minutes, the luciferase assay demonstrated a significant increase in survivability, increasing from 69.6 ± 0.048% in controls (pBK-vector) to 84.0 ± 0.080% in $K_V2.2$-expressing neurons (1-tailed paired t-test, P=0.049). C) Example confocal images of an individual neuron before, during and after 30 μM DTDP. Below, a schematic diagram of the experimental time course and conditions. We found that on average it took 86.67 ± 2.56 minutes for DTDP to significantly disrupt $K_V2.1$ somato-dendritic clusters (n=6, 2-tailed paired t-test, P=0.025). D) Bar graph summary of results, demonstrating that DTDP causes statistically significant disruption of $K_V2.1$ somato-dendritic clusters which is abolished by chelation of free Zn^{2+} by 10 μM TPEN. By approximately 1.5 hours following DTDP treatment the number of clusters/μM^2 decreased (0.090 ± 0.015 $K_V2.1$ clusters/$\mu M^2$30 μM DTDP n=14) compared to vehicle treated neurons (0.139 ± 0.017 $K_V2.1$ clusters/μM^2 0.01% DMSO n=10). A more pronounce disruption was noted at the 3+ hour time point in which whole cell voltage-clamp experiments were conducted (0.12 ± $K_V2.1$ clusters/μM^2 0.01% DMSO n= 16 versus 0.03 ± $K_V2.1$ clusters/μM^2 30 μM DTDP n=15). Removal of free Zn^{2+} by chelation, using 10 μM TPEN, completely abolished the effect (one-way ANOVA with Bonferonni post-hoc test, P=0.0004). E) (Top) Example whole cell voltage-clamp current density traces of neurons treated with either vehicle (0.01% DMSO) or DTDP (30 μM) 3–4.5 hours prior. (Bottom) bar graph summary demonstrating that the increase in $K_V2.1$ mediated current density observed in pBK-expressing controls (81.99 pA/pF ± 6.57, n=14 0.01% DMSO versus 171.88 pA/pF ± 18.72 pA/pF, n=15 30μM DTDP) was absent in cells expressing $K_V2.2CT$ (91.92 pA/pF ± 4.92, n=10 0.01% DMSO versus 83.34 pA/pF ± 11.19 n=7 30 μM DTDP; Kruskal-Wallis statistic 16.03, Dunn’s post-hoc test P=0.0011).

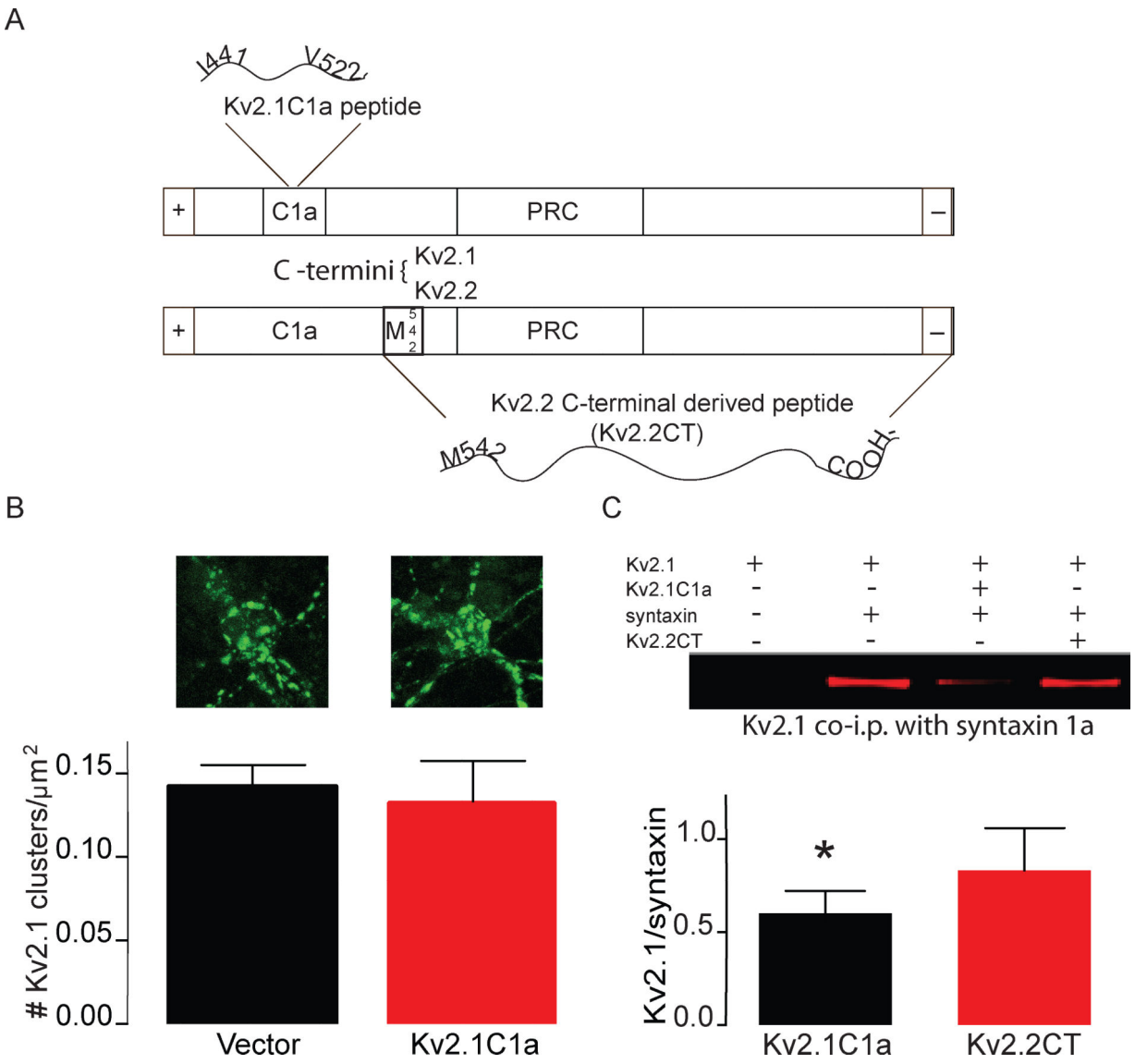

Figure 4. K_V2.2CT acts through a distinct mechanism that differs from K_V2.1C1a

A) Diagram illustrating the homology between the C-termini of K_V2.1 and K_V2.2 and the different non-overlapping domains that the K_V2.1C1a and K_V2.2CT proteins are derived from, both of which are neuroprotective against oxidative stress-inducing apoptosis. B) (top) Example confocal images of cortical neurons expressing K_V2.1-eGFP alone (left) and K_V2.1-eGFP+K_V2.1C1a (right) (bottom) Bar graph summary demonstrating that expression of K_V2.1C1a fails to disrupt K_V2.1 somato-dendritic clusters C) (top) Example Western blot of K_V2.1, co-immunoprecipitated with an anti-syntaxin primary antibody, comparing the effects of both K_V2.1C1a and K_V2.2CT on the association of syntaxin with K_V2.1 in Chinese hamster ovary cells. (Bottom) Bar graph summary of co-immunoprecipitation experiments demonstrating that only K_V2.1C1a causes a significant disassociation of K_V2.1 from syntaxin (1 sample t-test P=0.049, n=5).